

CheMixHub: Datasets and Benchmarks for Chemical Mixture Property Prediction

Ella Miray Rajaonson^{1,2}

Mahyar Rajabi Kochi¹

Luis Martin Mejía Mendoza³

Seyed Mohamad Moosavi^{1,2}

Benjamin Sanchez-Lengeling^{1,2}
ben.sanchez@utoronto.ca

¹ University of Toronto, Canada

² Vector Institute for Artificial Intelligence, Canada

³ Clean Energy Innovation Research Center, National Research Council, Canada

Abstract

Developing improved predictive models for multi-molecular systems is crucial, as nearly every chemical product used results from a mixture of chemicals. While being a vital part of the industry pipeline, the chemical mixture space remains relatively unexplored by the Machine Learning community. In this paper, we introduce CheMixHub, a holistic benchmark for molecular mixtures, covering a corpus of 11 chemical mixtures property prediction tasks, from drug delivery formulations to battery electrolytes, totalling approximately 500k data points gathered and curated from 7 publicly available datasets. CheMixHub introduces various data splitting techniques to assess context-specific generalization and model robustness, providing a foundation for the development of predictive models for chemical mixture properties. Furthermore, we map out the modelling space of deep learning models for chemical mixtures, establishing initial benchmarks for the community. This dataset has the potential to accelerate chemical mixture development, encompassing reformulation, optimization, and discovery. The dataset and code for the benchmarks can be found at: <https://github.com/chemcognition-lab/chemixhub>

1 Introduction

Mixtures of molecules are integral to our daily experiences: from the perfumes we smell [58] to the remedies we take [3, 74]. Understanding the interactions and behaviors of molecular mixtures is therefore essential for advancements in biochemistry [17], drug discovery [3] and environmental science [24]. Mixtures are particularly appealing because they offer greater flexibility in tailoring properties that specific application needs. By adjusting composition, substituting components, or introducing new ones, it is possible to fine-tune characteristics such as viscosity [6], volatility [19], stability [36], and conductivity [32]—features that are highly task-dependent. However, discovering new chemical mixtures, optimizing or reformulating them requires thorough characterization, which is time- and resource-intensive due to the exponentially growing number of candidate combinations. The mixture search space is vastly larger than that of single-component systems, making exhaustive experimental exploration impractical.

While Machine Learning (ML) has emerged as a powerful tool for accelerating the characterization and discovery of new materials [49], it faces unique challenges in the context of mixtures. On one hand, mixtures properties are highly correlated with strength of intermolecular interactions that cannot be inferred directly from the behavior of individual components. This causes quantitative

structure–property relationship (QSPR) modeling remain underexplored for multi-component systems compared to the substantial progress achieved for single-component systems [46]. On the other hand, the scarcity of publicly available datasets further limits progress in this area. While mono-molecular systems have benefited from well-established, community-driven datasets and benchmarks—such as MoleculeNet [68] and the Therapeutics Data Commons [25]—no centralized or standardized database currently exists for multi-component molecular systems.

In this paper, we introduce CHEMIXHUB, the first comprehensive benchmark of tasks for property prediction in chemical mixtures (see Figure 1). Covering 11 tasks across diverse chemical domains, CHEMIXHUB aims to enable systematic exploration of critical research questions, including:

1. What modeling strategies, particularly those exploiting permutation invariance and hierarchical structure, are most effective for mixtures?
2. Can a general-purpose representation generalize effectively across multiple mixture tasks?
3. To what extent does incorporating physics-based constraints improve model performance, particularly in varying experimental contexts like temperature?

Our key contributions, designed to facilitate the investigation of these questions, include:

- **Dataset curation:** Consolidating and standardizing 11 tasks from 7 datasets, reflecting the diversity and state of the chemical mixtures space.
- **New tasks:** Introducing two new tasks from a new dataset, curated from the IIThermo database (116,896 data points) and providing code to easily extend the curation to other target properties.
- **Generalization splits:** Implementing four distinct data splitting methodologies (random, unseen chemical component, varied mixture size/composition, and out-of-distribution context) to enable robust assessment of model generalization capabilities under various realistic scenarios.
- **Establishing baselines:** Benchmarking representative ML models to set initial performance levels and provide a comparative framework for future development.

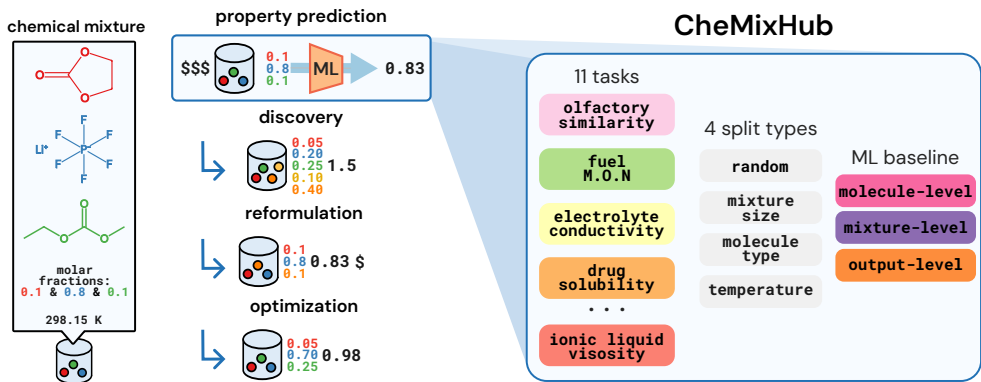


Figure 1: **CheMixHub: A benchmark for chemical mixture property prediction.** (Left) Illustrates a sample mixture input, including components and conditions. (Center) Highlights potential applications enabled by CheMixHub, such as reformulation, optimization, and discovery through property prediction. (Right) Summarizes CheMixHub’s structure: 11 tasks, 4 data split types, and a multi-level modeling baselines for comprehensive evaluation and development.

2 Related works

Chemical mixture properties datasets Various open-access and commercial sources offer experimental and computational mixture data, though these predominantly cover binary and ternary systems, with complex multi-component mixtures underrepresented (see Figure 2) [59, 44, 73, 34]. For instance, the open-source NIST ILThermo database [27] provides temperature-dependent transport and thermophysical properties for ionic liquid mixtures. Commercial platforms like DETHERM [67] and the Dortmund Data Bank [40] offer thermophysical data but are not publicly accessible. Despite these resources, substantial mixture data remains scattered throughout the literature, highlighting the need for unified datasets to enable robust mixture behavior modeling [80, 7, 14] and drive progress.

Deep learning on sets Predicting mixture properties from a set of components requires models that respect key inductive biases, notably permutation invariance [69] [23]. Many permutation-invariant set functions follow a common blueprint: a series of permutation-equivariant operations (e.g., element-wise MLPs or self-attention layers) followed by a permutation-invariant aggregation (e.g., summation or pooling) [8]. The pioneering *DeepSets* architecture [72, 41] exemplifies this, using an element-wise MLP and sum aggregation, followed by further non-linear processing (*sum-decomposition* [51, 56, 47, 64, 38, 82]). SetTransformer [33, 13] uses self-attention to model pairwise interactions with attention-based aggregation. Janossy pooling [39] offers another approach, explicitly modeling invariance and capturing higher-order interactions by averaging outputs over multiple input permutations [69, 78].

Learning on chemical mixtures ML is increasingly applied to chemical mixtures, primarily for property prediction, with emerging work on optimization and discovery [81, 53]. Common strategies involve aggregating molecular-level chemo-informatic features, graph neural networks (GNNs) embeddings [54, 75, 58, 80, 6] or large pre-trained chemical language models (CLMs) [55, 45]—using a *DeepSets*-like architecture. Alternatively, mixture representations are formed by weighted combinations of individual component descriptors [54, 55, 45], or learned by tree-based models from these descriptors [3]. A separate line of research explores attention-based architectures [75, 58]. Some work explicitly models pairwise interaction terms between mixture components, offering a more physically grounded and expressive representation [80]. These mixture embeddings are then fed to predictive models like neural networks [6], gradient boosting machines [3], or Gaussian processes [53].

3 Datasets

3.1 Dataset overview

We curated 11 regression tasks from 7 published datasets across the chemical mixture literature, which are summarized in Table 1. The tasks were selected based on application domain and prior use as baselines in ML studies. To ensure their accessibility and standardization for ML applications, we provide a Croissant [2] file detailing their metadata, structure, and semantics based on schema.org. The dataset licenses are listed in Section A.1.

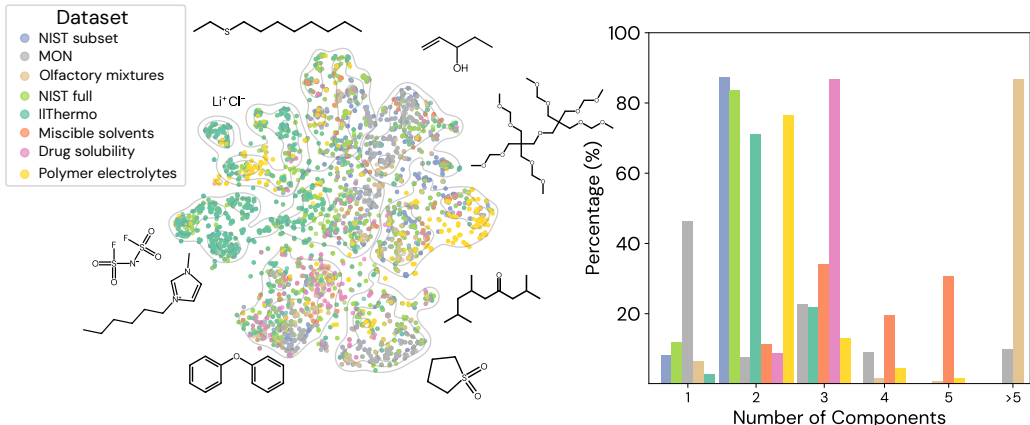


Figure 2: **Diversity of Chemical Structures and Mixture Compositions in CheMixHub.** (Left) t-SNE visualization of the molecular structural diversity, with points colored by their source dataset. (Right) Histogram showing the percentage of mixtures based on their number of components.

3.2 Tasks

Miscible Solvents (3 tasks) Homogeneous solutions are important in a variety of material science applications such as battery electrolytes, chemical reactivity, and consumer packaged goods. The Miscible Solvents dataset is a set of three tasks centered around miscible solvent properties, originally generated by Chew et al. using molecular dynamics (MD) simulations for 19,238 unique mixtures [14].

Table 1: **CheMixHub tasks summary.** *T* indicates Temperature dependency. *Mole Fractions* indicates if mole fractions of the mixture components are available. *Arrhenius relationship* indicates if the task can be modeled using the Arrhenius equation. *Exp.* indicates if the data was obtained from wet-lab experiments or simulations.

Tasks	Units	Datapoints	Max # Components	# Unique Mixtures	# Unique Molecules	Mixture Context	Mole Fractions	Arrhenius Relationship	Exp.
Miscible solvents	ρ	g/m ³	30,142	5	19,238	81	—	✓	✗
	ΔH_{mix}	kJ/mol	30,142	5	19,238	81	—	✓	✗
	ΔH_{vap}	kcal/mol	30,142	5	19,238	81	—	✓	✗
ILThermo	$\ln(\kappa)$	S/m	40,904	3	14,438	479	T	✓	✓
	$\ln(\eta)$	Pa-s	75,992	3	15,878	699	T	✓	✓
NIST	$\ln(\eta_{source})$	cP	239,201	2	84,133	1648	T	✓	✓
	$\ln(\eta_{mixprop})$	cP	34,374	2	4566	1397	T	✓	✓
Drug solubility	$\ln(S)$	g/100g	27,166	3	3259	169	T	✓	✗
Solid Polymer Electrolyte	$\ln(\kappa)$	S/m	11,350	5	1749	402	T	✓	✗
Olfactory similarity	—	—	865	43	743	201	—	✗	✗
Motor Octane Number (MON)	—	—	684	121	352	419	—	✓	✗

- **Density (ρ):** ρ measures how tightly packed the molecules are for a mixture. In industrial applications, density is important as it dictates the final weight and polarity of the product.
- **Heat of vaporization (ΔH_{vap}):** ΔH_{vap} is the amount of heat needed to convert some fraction of liquid into vapor. While experimentally measuring ΔH_{vap} for mixtures is challenging, it effectively measures the cohesion energy of a liquid and has been previously observed to correlate with temperature-dependent viscosity [15].
- **Enthalpy of mixing (ΔH_m):** ΔH_m is a fundamental thermodynamic property of liquid mixtures that measures the energy released or absorbed upon the mixing of pure components into a single phase in equilibrium. It is important for process design that dictates properties, such as solubility and phase stability.

ILThermo (2 tasks) Ionic liquids (ILs) are salts composed of organic cations and organic or inorganic anions that remain liquid at temperatures below 100 °C [1, 61, 79]. ILThermo is a web-based database that provides extensive information on over 50 chemical and physical properties of pure ILs, as well as their binary and ternary mixtures with various solvents [28]. For the scope of this paper, we selected two property prediction tasks from ILThermo; however, we have open-sourced our curation code to facilitate the addition of further tasks in the future. Details of the curation process are provided in Section A.7, and the selected tasks are summarized below:

- **Ionic conductivity (κ):** Higher κ makes ILs attractive for use as electrolytes in energy storage and other electrochemical applications [37]. However, ionic conductivity of ionic liquid mixtures is a complex phenomenon and is influenced by multiple factors such as size and charge on the ions, polarity and dielectric strength of the solvent, viscosity, hydrogen bonding strength, ion association, etc [57]. To facilitate data-driven approaches, ILThermo dataset includes 40,904 κ data points curated from literature, covering 14,438 unique mixtures composed of 479 molecules.
- **Viscosity (η):** Modeling the viscosity of ILs is particularly challenging, as their viscosity can be orders of magnitude higher than those of conventional solvents [43]. This complexity arises from the coexistence of multiple interaction types—ionic, dispersion, dipole-dipole, and induced dipole interactions—that are more pronounced compared to typical organic solvents. The ILThermo dataset provides 75,992 viscosity (η) data points curated from the literature, encompassing 15,878 unique mixtures formed from 699 distinct molecules.

NIST viscosity (2 task) Dynamic viscosity is a key design objective for modern process engineering and products. However, modeling the viscosity of liquid mixtures presents significant challenges due to the complex molecular interactions and the potential for nonmonotonic behavior [50]. NIST Thermodynamics Research Center (TRC) data archival system provides one of the most comprehensive datasets containing 239,201 dynamic viscosity datapoints of binary liquid mixtures [27]. Bilodeau et al. proposed a smaller version of the dataset by applying two key preprocessing steps: (1) removing data entries with SMILES strings containing multiple, non-covalently bonded fragments, and (2) excluding entries where either molecule was predicted to be a gas or solid in its pure form. These steps reduced the dataset to 34,374 data points[6].

Drug solubility (1 task) The drug solubility in mixture of solvents is a critical factor that influences various stages of the pharmaceutical development pipeline, from drug discovery, drug analysis to

formulation design. It allows greater flexibility through adjusting solvent combinations and ratios enabling solubility to be tailored to meet specific needs and to co-dissolve other necessary materials. The drug solubility dataset originally curated by Bao et al. from literature includes 27,166 data points [3]

Solid polymer electrolytes conductivity (1 task) Solid polymer electrolytes (SPEs), proposed as potential replacements for conventional liquid organic electrolytes in batteries, have been engineered to offer improved electrochemical stability and reduced flammability. However, their practical use is limited by inherently low ionic conductivity. To support data-driven research on this issue, Bradford et al. compiled a dataset from the literature comprising 11,350 ionic conductivity measurements across more than 1,700 unique electrolyte formulations. Each formulation is uniquely defined by the polymer, salt, salt concentration, polymer molecular weight, and any additives present [7].

Motor Octane Number (1 task) Kuzhagaliyeva et al. compiled a database containing 684 data points for 352 unique single hydrocarbons and mixtures, reporting experimentally measured motor octane numbers (MON) from various literature sources. MON is a combustion-related property commonly used to assess a fuel’s resistance to knocking. The dataset is categorized into three subpopulations: pure components, blends with 10 or fewer components (mostly surrogates), and complex fuels containing more than 10 components [31].

Olfactory similarity (1 task) The dataset was originally compiled from previous publications [66, 52, 9] by Tom et al. [58]. Data for each of these publications was obtained from pyrFume [11] and consists of 865 pairwise mixture comparisons. Each pair is assigned a continuous perceptual similarity score ranging from 0 (completely similar) to 1 (completely different). This final score represents an average of similarity ratings obtained from human participants across different experimental paradigms.

3.3 Curation pipeline

The following points highlight data set design choices we made:

- **Handling of chemical species diversity** The diversity of the chemical-mixture space extends beyond fields of applications to the fundamental level of chemical representation itself. Indeed, different chemical moieties for which representations may not have been as explored digitally as small-molecules may be encountered (e.g. polymers) in some mixtures but not in others. In CHEMIXHUB, a wide range of chemical species is present (see Figure 2) spanning salts and polymers. This diversity should be taken into account when modeling mixtures, the correct representation is still an open problem. All the chemical species in this datasets can be expressed as a SMILES string, which are standardized using RDKit. Polymers are represented by their monomeric units, along with their Mass average molar mass (M_W) or Number average molar mass (M_N). Molecules with ionic bonding (salts) are preserved and flagged in the dataset.
- **Number of components** While our focus is on multi-component systems, we preserve the single-component data points in the datasets with the exception of IIThermo. We leave the choice to the user to filter out single-component data points in CHEMIXHUB.
- **Representing mixture composition** All possible compositional ratio were converted to mole fractions, discarding data points that did not have the information to make that conversion.
- **Missing temperature values** Standard conditions (298.15K) are assumed if temperature values are not reported. For the datasets where this is the case, added values are flagged. This flag can optionally be passed to the model for it to implicitly learn uncertainty over those assumed values.
- **Data scales** Due to great variations in experimental value ranges, it is common to apply logarithmic scaling to conductivity, solubility and viscosity properties [6, 7, 3]. We follow this principle and apply it to these types of properties.

3.4 Dataset splitting strategies

Aside from traditional random cross-validation (CV) splits with a default of 5-fold 70/10/20 training/validation/test splits, we propose 3 additional splitting strategies for benchmarking, to explore generalization capabilities of models:

- **Mixture size splits:** For a given threshold, the training set only contains mixtures with components that have a number of components less than the threshold, and the test set contains only mixtures that are above the threshold. For the olfactory similarity task, we employ the geometric mean of

the two mixtures. This setting is interesting in industry because we want to predict the properties of complex mixtures while training on simpler, cheaper ones.

- **Leave-molecules-out (LMO) splits:** The test sets are split from the dataset such that certain molecules will not appear in the training set. Studying new molecules is an important consideration when validating models to ensure the model is applicable in out of distribution molecular discovery settings.
- **Temperature splits:** As highlighted in Table 1, multiple tasks in CHEMIXHUB have a temperature dependency. It is also desirable for industry to be able to predict the properties of certain mixtures in different temperature ranges than the training one. We bin the temperature range in 5 categories based on the temperature distribution observed across the 11 tasks and use the bins as a 5-fold split.

4 Benchmark

4.1 Modeling space

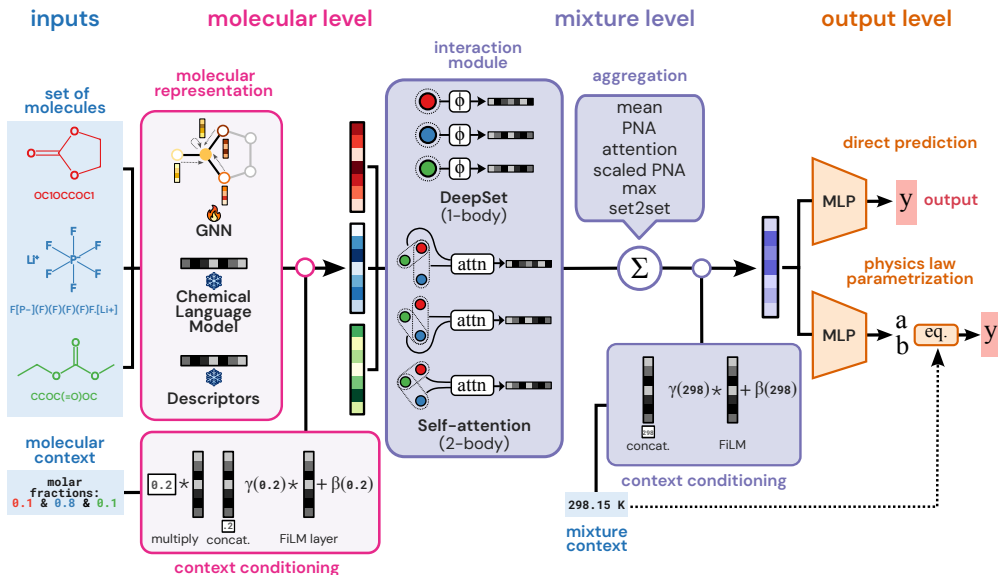


Figure 3: **Mapping out the deep learning modeling space for chemical mixtures.** We highlight three levels: (1) molecular representation and context infusion (e.g., molecular fraction), (2) mixture-level interaction aggregation, and infusion of global mixture context (e.g., temperature), (3) property output generation, each offering distinct avenues for model development.

The inherent set-like structure of molecular mixtures mandates that deep learning models incorporate specific inductive biases. Primarily, models must ensure permutation invariance, meaning the predicted property remains unaffected by the input order of constituent molecules and their compositions. Additionally, they must be flexible to a varying number of input components, allowing, for example, a model trained on binary mixtures to generalize to ternary systems or more complex formulations. These symmetries are critical for downstream applications where industrial formulations rely on precise compositions, ingredients are combined without a fixed order, and the effects of component addition or removal are routinely assessed.

To guide model development, we define a structured modeling space (Figure 3) that operates on input mixture data. Each data point comprises a set of pure component molecules, their associated molecular context (e.g., mole fractions), and the overall mixture context (e.g., temperature). This space, while focusing on foundational one-body and pairwise interactions and various aggregation operations, is non-exhaustive; future work could explore explicit N-body interactions or more sophisticated set-to-vector encoding mechanisms. Conceptually, this modeling space is divided into three levels: 1) molecular representation, 2) mixture representation, and 3) output generation.

Molecular representation level We benchmark three common embedding techniques: GNNs, CLMs and molecular descriptors. For GNNs, we use a GRAPHNETS architecture [4] trained end-to-end with the other module to learn the embeddings during the task (details in Section A.2), while for CLMs we rely on frozen pre-trained representations from MOLT5 [18]. All training is performed using the Adam optimizer [30]. Cheminformatics molecular descriptors are normalized 200 dimensional from RDKit obtained from DESCRIPTASTORUS [29]. After obtaining the molecular embeddings, we consider three different ways of infusing the molecular context into them: 1) element-wise multiplication, 2) concatenation, 3) feature-wise linear modulation (FiLM) layer [42].

Mixture representation level We explore two possible interaction modules: DeepSets [72] and self-attention [60], which can be thought of as enabling one-body and two-body interactions between molecules in the mixture, respectively. We consider six different types of permutation invariant aggregation operations: mean, max, attention-based aggregation [60], principal neighborhood aggregation (PNA) [16], PNA scaled according to the number of component in the mixture and set2set [63] which yields the mixture embedding. We then consider two different ways of incorporating the mixture context into it: 1) concatenation 2) using a FiLM layer.

Output level We consider using either a fully-connected predictive head that directly outputs a predicted value, or for tasks that consists in predicting properties which are temperature dependent, predicting the parameters of the Arrhenius equation which is then used to determine the final outputted value (see Section 4.4).

Baseline To establish a strong non-deep learning baseline, we provide comparison with a gradient-boosted random forest model, XGBoost [12] using RDKit descriptors or MOLT5 embeddings molecular features. These features are linearly combined with their respective molecular context and then concatenated with the overall mixture context to form the input for XGBoost (details in Section A.6).

4.2 Performances across tasks

Table 2: **Model performances across CHEMIXHUB tasks** Reported MAE (\downarrow) on 5-fold random CV splits. The mean and standard deviation are reported.

Molecular rep.	Mixture rep.	Miscible Solvents			Drug Solubility $\ln(S)$	SPE $\ln(\kappa)$	NIST-full $\ln(\eta)$
		ρ	ΔH_{mix}	ΔH_{vap}			
GNN	Attention	0.018 ± 0.020	0.158 ± 0.002	0.098 ± 0.006	0.087 ± 0.006	0.312 ± 0.043	0.136 ± 0.010
	Deepsets	0.003 ± 0.000	<u>0.159 ± 0.002</u>	0.406 ± 0.668	0.065 ± 0.005	0.315 ± 0.067	0.131 ± 0.010
MolT5	XGB	0.009 ± 0.000	0.269 ± 0.004	0.306 ± 0.003	0.028 ± 0.001	0.222 ± 0.007	0.148 ± 0.001
	Attention	0.005 ± 0.001	0.157 ± 0.002	0.125 ± 0.077	0.082 ± 0.027	0.279 ± 0.006	0.076 ± 0.004
	Deepsets	<u>0.008 ± 0.005</u>	<u>0.157 ± 0.003</u>	0.071 ± 0.002	0.130 ± 0.013	0.328 ± 0.010	0.162 ± 0.009
RDKit	XGB	0.009 ± 0.000	0.225 ± 0.005	0.295 ± 0.002	0.028 ± 0.001	<u>0.223 ± 0.008</u>	0.055 ± 0.000
	Attention	0.006 ± 0.001	0.167 ± 0.002	0.199 ± 0.030	0.070 ± 0.006	0.394 ± 0.028	0.069 ± 0.006
	Deepsets	0.005 ± 0.000	0.207 ± 0.008	0.079 ± 0.005	0.179 ± 0.011	0.344 ± 0.016	0.137 ± 0.005
Molecular rep.	Mixture rep.	ITThermo		MON MON	NIST $\ln(\eta)$	Olfaction	
		$\ln(\kappa)$	$\ln(\eta)$			Mixture similarity	
GNN	Attention	0.276 ± 0.044	0.154 ± 0.084	10.240 ± 1.658	<u>0.035 ± 0.004</u>	0.129 ± 0.005	
	Deepsets	0.226 ± 0.017	0.206 ± 0.020	5.990 ± 1.382	0.091 ± 0.005	0.146 ± 0.010	
MolT5	XGB	0.071 ± 0.001	<u>0.078 ± 0.002</u>	5.002 ± 0.538	0.059 ± 0.001	0.128 ± 0.006	
	Attention	0.244 ± 0.011	<u>0.083 ± 0.035</u>	<u>4.660 ± 0.603</u>	0.030 ± 0.001	<u>0.123 ± 0.005</u>	
	Deepsets	0.196 ± 0.013	0.132 ± 0.003	5.296 ± 0.585	0.056 ± 0.004	0.121 ± 0.006	
RDKit	XGB	<u>0.073 ± 0.002</u>	0.076 ± 0.002	4.570 ± 0.348	0.048 ± 0.002	0.125 ± 0.006	
	Attention	<u>0.407 ± 0.019</u>	0.100 ± 0.003	11.297 ± 2.110	0.056 ± 0.004	0.148 ± 0.010	
	Deepsets	0.290 ± 0.059	0.107 ± 0.007	7.625 ± 1.874	0.047 ± 0.003	0.150 ± 0.008	

We investigate how the architectural considerations highlighted in Section 4.1 impact the predictive power of models across the 11 tasks in CHEMIXHUB. We first select the best performing architectures that covers all combinations of molecular representation and mixture interaction modules (6 models) by a Bayesian optimization hyperparameter search (details in section A.5) on each task. Then, we train and test the selected model on 5-fold random CV splits (70/10/20 training/validation/test split). We report results across mean absolute error (MAE). The results compiled from the CV splits for all

models evaluated are tabulated in Table 8. Additional metrics (Pearson correlation coefficient ρ and Kendall ranking coefficient τ) are reported in Section A.8.

We observe that traditional tree-based methods like XGBOOST are robust baselines on a great variety of tasks. It is interesting to note that XGBOOST-based methods greatly struggle on predicting ΔH_{mix} and ΔH_{vap} , two properties well known for their non-linear mixture behavior. Overall, we observe pre-trained representations of CLMs like MOLT5 tend to yield better performances across our dataset compared to GNN-based representation and cheminformatics descriptors. We believe that pre-training on related data would greatly improve the performances of GNNs, as it has been shown to in the literature [58, 54]. Regarding the choice of mixture interaction module, the need for higher level of interactions tend to be task-dependent, with no consistent advantage of one method over the other.

4.3 Generalization to new mixture sizes and molecules

We further study how robust models are to variation in the number of components in mixtures and to new molecular entities. For the scope of this study, we focus on the datasets which have the greatest variation in terms of number of components, namely the MON and Olfactory similarity datasets. We assess the performance of the best deep learning model for each task as determined in Section 4.2 and report it using the Pearson correlation coefficient ρ in Figure 4.

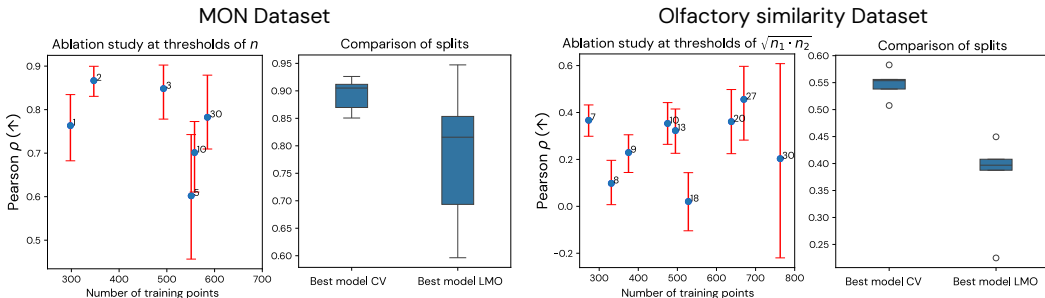


Figure 4: **Generalization to new mixture sizes and molecules.** For each dataset: (Left) Ablation study with training data only containing mixtures with (geometric) average number of molecules less than a threshold. The thresholds are indicated for each split. (Right) Boxplot of the best deep learning model test Pearson correlation on random CV splits, and the LMO splits.

We observe great sensitivity to mixture sizes across both datasets. We hypothesize that addition of new datapoints with slightly higher numbers of components may be considered as noise by the model and therefore leads to overfitting. Additionally, we observe a significant decrease in performance when considering new chemistries. This lack of extrapolative behavior regarding individual molecular species is expected, as we noted that the molecular level modeling plays an essential part in model performance.

4.4 Explicit physics-based modeling

Previous work have reported that incorporating known physical or chemical constraints into ML models can improve accuracy and generalizability of model predictions [7, 80]. We investigate how swapping a regular fully connected predictive head for a “physics-based” predictive head impacts the model’s performance. Namely, we modify the predictive head to output the coefficients of a physics law suitable for the task. For the scope of this paper, we limit our study to temperature-dependent tasks whose target property can be effectively modeled by the Arrhenius equation.

$$\ln(y) = \ln(A) - \frac{E_a}{RT} \quad (1)$$

where y can be viscosity η and ionic conductivity κ tasks, R is the perfect gas law constant, T is the given temperature and A and E_a parameters to predict. We assess the performance of the best deep learning model for each task, as determined in Section 4.2 and conduct the study on temperature dependent splits to investigate generalizability to new temperature ranges. We also report the performance of XGBOOST on this harder type of split.

We observe that adding a physics bias via the Arrhenius equation greatly improves the performance of deep learning architectures in this setting. This technique also allows better interpretability of the

predictive model, as it grounds it in known equations. Additionally, we note that the performance of XGBOOST, a model that typically performs well on randomized splits, has significantly decreased performance when evaluated on a harder and more realistic split, highlighting the importance of generalizability assessment and not relying on a single split to report in literature.

Table 3: **Physics bias improves performances across temperature-dependent tasks** Reported on temperature range exclusion splits, up to 5-fold. The mean and standard deviation are reported.

Metric	Model	ITThermo		NIST	SPE
		$\ln(\kappa)$	$\ln(\eta)$	$\ln(\eta)$	$\ln(\kappa)$
MAE (\downarrow)	Best XGB	0.386 ± 0.142	0.432 ± 0.160	0.126 ± 0.022	0.482 ± 0.138
	Best model	0.354 ± 0.152	0.162 ± 0.096	0.079 ± 0.006	0.481 ± 0.228
	Best model + Arrhenius	0.284 ± 0.025	0.127 ± 0.011	0.048 ± 0.013	0.363 ± 0.015
Pearson ρ (\uparrow)	Best XGB	0.940 ± 0.056	0.941 ± 0.063	0.877 ± 0.008	0.935 ± 0.018
	Best model	0.923 ± 0.084	0.968 ± 0.033	0.946 ± 0.006	0.941 ± 0.024
	Best model + Arrhenius	0.987 ± 0.002	0.988 ± 0.003	0.980 ± 0.011	0.961 ± 0.003

5 Conclusion

In this study, we introduced CHEMIXHUB, a comprehensive suite of datasets and benchmarks designed to accelerate research in chemical mixture property prediction. Addressing the critical need for standardized resources in a field characterized by scattered datasets, inconsistent evaluation protocols, and limited open-source model implementations, CHEMIXHUB provides a curated collection of 11 tasks, diverse splitting strategies for robust generalization assessment, and initial baselines using representative ML models. Our work aims to lower the barrier to entry and foster systematic progress in understanding and modeling these complex multi-molecular systems.

Our benchmarking revealed that traditional models like XGBoost with appropriate chemical features offer strong baselines on random splits, often rivaling more complex deep learning methods. This highlights the necessity for deep learning approaches to demonstrate clear advantages, particularly on more challenging out-of-distribution tasks. We observed that datasets with greater monomolecular diversity (e.g., MON, Olfactory Similarity) benefit from hierarchical modeling as well as tasks with well known non-linear relationships, such as enthalpy of mixing ΔH_{mix} and heat of vaporization ΔH_{vap} , underscoring the need for advanced modeling and rigorous evaluation beyond simple random splits. Encouragingly, the explicit incorporation of physics-based constraints, like the Arrhenius equation for temperature-dependent properties, significantly enhanced model performance and generalization, suggesting a fruitful direction for future work in fusing domain knowledge with data-driven techniques. The optimal level of interaction modeling—whether one-body (*DeepSets*-like) or explicit many-body approaches—also remains task-dependent and warrants further investigation, alongside innovations in aggregation, context conditioning, and attention mechanisms tailored for mixtures.

CHEMIXHUB is intended to catalyze progress across these diverse research frontiers, equipping the community to tackle the complex and impactful domain of chemical mixture modeling for better drugs and materials. We condemn any malicious use of our work to create malicious or hazardous chemicals.

6 Limitations

Several limitations of current approaches and avenues for future research are illuminated by CHEMIXHUB. Representing complex entities like polymers, currently simplified to monomeric units, requires more sophisticated featurization. Beyond property prediction, the vast chemical mixture space invites exploration into formulation discovery, optimization, and de novo design. These endeavors, especially those involving iterative experimental design, are nascent and present significant ML challenges, particularly given the often data-scarce nature of experimental mixture datasets. Thus, techniques for data-efficient learning, multi-task approaches, and robust pre-training strategies are crucial. While the GNNs in our study were not pre-trained, exploring task-specific or general pre-training for mixture-aware GNNs or CLMs is a promising direction. Finally, enhancing model interpretability—providing insights at both molecular and mixture interaction levels—is essential for the practical adoption of these models in chemical research and industry.

Acknowledgments and Disclosure of Funding

E. M. R. and B. S.-L. would like to thank Prof. Alán Aspuru-Guzik for his support and advice. This research was enabled in part by computational resources provided by the Digital Research Alliance of Canada (<https://alliancecan.ca>) and the Acceleration Consortium (<https://acceleration.utoronto.ca>). The authors gratefully acknowledge financial support from the Acceleration Consortium, the Natural Sciences and Engineering Council of Canada (NSERC), University of Toronto’s Data Science Institute and the Vector Institute.

References

- [1] M. Aghaie, N. Rezaei, and S. Zendejboudi. A systematic review on co2 capture with ionic liquids: Current status and future prospects. *Renewable and sustainable energy reviews*, 96:502–525, 2018.
- [2] M. Akhtar, O. Benjelloun, C. Conforti, P. Gijssbers, J. Giner-Miguel, N. Jain, M. Kuchnik, Q. Lhoest, P. Marcenac, M. Maskey, P. Mattson, L. Oala, P. Ruyssen, R. Shinde, E. Simperl, G. Thomas, S. Tykhonov, J. Vanschoren, J. van der Velde, S. Vogler, and C.-J. Wu. Croissant: A metadata format for ml-ready datasets. DEEM ’24, page 1–6, New York, NY, USA, 2024. Association for Computing Machinery.
- [3] Z. Bao, G. Tom, A. Cheng, J. Watchorn, A. Aspuru-Guzik, and C. Allen. Towards the prediction of drug solubility in binary solvent mixtures at various temperatures using machine learning. *Journal of Cheminformatics*, 16(1):117, 2024.
- [4] P. W. Battaglia, J. B. Hamrick, V. Bapst, A. Sanchez-Gonzalez, V. Zambaldi, M. Malinowski, A. Tacchetti, D. Raposo, A. Santoro, R. Faulkner, et al. Relational inductive biases, deep learning, and graph networks. *arXiv preprint arXiv:1806.01261*, 2018.
- [5] L. Biewald. Experiment tracking with weights and biases, 2020. Software available from wandb.com.
- [6] C. Bilodeau, A. Kazakov, S. Mukhopadhyay, J. Emerson, T. Kalantar, C. Muzny, and K. Jensen. Machine learning for predicting the viscosity of binary liquid mixtures. *Chemical Engineering Journal*, 464:142454, 2023.
- [7] G. Bradford, J. Lopez, J. Ruza, M. A. Stolberg, R. Osterude, J. A. Johnson, R. Gomez-Bombarelli, and Y. Shao-Horn. Chemistry-informed machine learning for polymer electrolyte discovery. *ACS Central Science*, 9(2):206–216, 2023.
- [8] M. M. Bronstein, J. Bruna, T. Cohen, and P. Veličković. Geometric deep learning: Grids, groups, graphs, geodesics, and gauges, 2021.
- [9] C. Bushdid, M. O. Magnasco, L. B. Vosshall, and A. Keller. Humans can discriminate more than 1 trillion olfactory stimuli. *Science*, 343(6177):1370–1372, 2014.
- [10] E. A. Cade, D. R. Saeva, and M. M. Hoffmann. Comparing composition-and temperature-dependent excess molar volumes of binary systems involving ionic liquids. *Journal of Chemical & Engineering Data*, 59(6):1892–1914, 2014.
- [11] J. B. Castro, T. J. Gould, R. Pellegrino, Z. Liang, L. A. Coleman, F. Patel, D. S. Wallace, T. Bhatnagar, J. D. Mainland, and R. C. Gerkin. Pyrfume: A window to the world’s olfactory data. *bioRxiv*, pages 2022–09, 2022.
- [12] T. Chen and C. Guestrin. Xgboost: A scalable tree boosting system. In *Proceedings of the 22nd acm sigkdd international conference on knowledge discovery and data mining*, pages 785–794, 2016.
- [13] Z. Chen, X. Zhu, D. Su, and J. C. Chuang. Stacking deep set networks and pooling by quantiles. In *Forty-first International Conference on Machine Learning*, 2024.
- [14] A. K. Chew, M. A. F. Afzal, Z. Kaplan, E. M. Collins, S. Gattani, M. Misra, A. Chandrasekaran, K. Leswing, and M. D. Halls. Leveraging high-throughput molecular simulations and machine learning for the design of chemical mixtures. 2025.

- [15] A. K. Chew, M. Sender, Z. Kaplan, A. Chandrasekaran, J. Chief Elk, A. R. Browning, H. S. Kwak, M. D. Halls, and M. A. F. Afzal. Advancing material property prediction: using physics-informed machine learning models for viscosity. *Journal of Cheminformatics*, 16(1):31, 2024.
- [16] G. Corso, L. Cavalleri, D. Beaini, P. Liò, and P. Veličković. Principal neighbourhood aggregation for graph nets. *Advances in neural information processing systems*, 33:13260–13271, 2020.
- [17] C. D. Derby, T. S. McClintock, and J. Caprio. Understanding responses to chemical mixtures: looking forward from the past. *Chemical senses*, 47:bjac002, 2022.
- [18] C. Edwards, T. Lai, K. Ros, G. Honke, K. Cho, and H. Ji. Translation between molecules and natural language. *arXiv preprint arXiv:2204.11817*, 2022.
- [19] S. Evjen, R. Wanderley, A. Fiksdahl, and H. K. Knuutila. Viscosity, density, and volatility of binary mixtures of imidazole, 2-methylimidazole, 2, 4, 5-trimethylimidazole, and 1, 2, 4, 5-tetramethylimidazole with water. *Journal of Chemical & Engineering Data*, 64(2):507–516, 2019.
- [20] S. Falkner, A. Klein, and F. Hutter. Bohb: Robust and efficient hyperparameter optimization at scale. In *International conference on machine learning*, pages 1437–1446. PMLR, 2018.
- [21] X. Fan, X. Ji, L. Chen, J. Chen, T. Deng, F. Han, J. Yue, N. Piao, R. Wang, X. Zhou, et al. All-temperature batteries enabled by fluorinated electrolytes with non-polar solvents. *Nature Energy*, 4(10):882–890, 2019.
- [22] K. L. Gering. Prediction of electrolyte conductivity: results from a generalized molecular model based on ion solvation and a chemical physics framework. *Electrochimica Acta*, 225:175–189, 2017.
- [23] A. Goyal and Y. Bengio. Inductive biases for deep learning of higher-level cognition. *Proceedings of the Royal Society A*, 478(2266):20210068, 2022.
- [24] K. A. Heys, R. F. Shore, M. G. Pereira, K. C. Jones, and F. L. Martin. Risk assessment of environmental mixture effects. *RSC advances*, 6(53):47844–47857, 2016.
- [25] K. Huang, T. Fu, W. Gao, Y. Zhao, Y. Roohani, J. Leskovec, C. W. Coley, C. Xiao, J. Sun, and M. Zitnik. Therapeutics data commons: Machine learning datasets and tasks for drug discovery and development. *Proceedings of Neural Information Processing Systems, NeurIPS Datasets and Benchmarks*, 2021.
- [26] Ivan Chernyshov. Ilthermopy: Python api for the ilthermo 2.0 database.
- [27] A. Kazakov, C. D. Muzny, K. Kroenlein, V. Diky, R. D. Chirico, J. W. Magee, I. M. Abdulagatov, and M. Frenkel. Nist/trc source data archival system: The next-generation data model for storage of thermophysical properties. *International Journal of Thermophysics*, 33:22–33, 2012.
- [28] A. F. Kazakov, J. W. Magee, R. D. Chirico, V. Diky, K. G. Kroenlein, C. D. Muzny, and M. D. Frenkel. Ionic liquids database-ilthermo (v2. 0). 2013.
- [29] B. Kelley et al. GitHub - bp-kelley/descriptastorus: Descriptor computation (chemistry) and (optional) storage for machine learning, 2024.
- [30] D. P. Kingma. Adam: A method for stochastic optimization. *arXiv preprint arXiv:1412.6980*, 2014.
- [31] N. Kuzhagaliyeva, S. Horváth, J. Williams, A. Nicolle, and S. M. Sarathy. Artificial intelligence-driven design of fuel mixtures. *Communications Chemistry*, 5(1):111, 2022.
- [32] G. Latini, G. Passerini, F. Polonara, and G. Vitali. Alternative refrigerants in the liquid phase: thermal conductivity of binary and ternary mixtures. 1996.
- [33] J. Lee, Y. Lee, J. Kim, A. Kosiorek, S. Choi, and Y. W. Teh. Set transformer: A framework for attention-based permutation-invariant neural networks. In *International conference on machine learning*, pages 3744–3753. PMLR, 2019.

- [34] D. Li, X. Zhang, C. Xin, and M. Liu. Thermophysical and excess properties of binary mixtures of dibutyl ether and components of biodiesel. *Journal of Solution Chemistry*, 54(1):125–139, 2025.
- [35] M. Lifi, N. Munoz-Rujas, E. A. Montero, Y. Chhiti, F. Aguilar, and F. E. M’hamdi. Alaoui. Measurement and modeling of excess molar enthalpies of binary mixtures involving hydrocarbon components of fuel. *Journal of Chemical & Engineering Data*, 65(2):717–724, 2020.
- [36] J. Liu, Y. Liu, C. Liu, L. Xin, and W. Yu. Experimental and theoretical study on thermal stability of mixture r1234ze (e)/r32 in organic rankine cycle. *Journal of Thermal Science*, 32(4):1595–1613, 2023.
- [37] X. Liu, A. Mariani, H. Adenusi, and S. Passerini. Locally concentrated ionic liquid electrolytes for lithium-metal batteries. *Angewandte Chemie International Edition*, 62(17):e202219318, 2023.
- [38] H. Maron, O. Litany, G. Chechik, and E. Fetaya. On learning sets of symmetric elements. In *International conference on machine learning*, pages 6734–6744. PMLR, 2020.
- [39] R. L. Murphy, B. Srinivasan, V. Rao, and B. Ribeiro. Janossy pooling: Learning deep permutation-invariant functions for variable-size inputs. *arXiv preprint arXiv:1811.01900*, 2018.
- [40] U. Onken, J. Rarey-Nies, and J. Gmehling. The dortmund data bank: A computerized system for retrieval, correlation, and prediction of thermodynamic properties of mixtures. *International Journal of Thermophysics*, 10:739–747, 1989.
- [41] Z. Ou, T. Xu, Q. Su, Y. Li, P. Zhao, and Y. Bian. Learning neural set functions under the optimal subset oracle. *Advances in Neural Information Processing Systems*, 35:35021–35034, 2022.
- [42] E. Perez, F. Strub, H. De Vries, V. Dumoulin, and A. Courville. Film: Visual reasoning with a general conditioning layer. In *Proceedings of the AAAI conference on artificial intelligence*, volume 32, 2018.
- [43] F. Philippi, D. Rauber, K. L. Eliassen, N. Bouscharain, K. Niss, C. W. Kay, and T. Welton. Pressing matter: why are ionic liquids so viscous? *Chemical Science*, 13(9):2735–2743, 2022.
- [44] A. Podgorsek, J. Jacquemin, A. Pádua, and M. Costa Gomes. Mixing enthalpy for binary mixtures containing ionic liquids. *Chemical reviews*, 116(10):6075–6106, 2016.
- [45] I. Priyadarsini, V. Sharma, S. Takeda, A. Kishimoto, L. Hamada, and H. Shinohara. Improving performance prediction of electrolyte formulations with transformer-based molecular representation model. *arXiv preprint arXiv:2406.19792*, 2024.
- [46] E. O. Pyzer-Knapp, J. W. Pitera, P. W. Staar, S. Takeda, T. Laino, D. P. Sanders, J. Sexton, J. R. Smith, and A. Curioni. Accelerating materials discovery using artificial intelligence, high performance computing and robotics. *npj Computational Materials*, 8(1):84, 2022.
- [47] C. R. Qi, H. Su, K. Mo, and L. J. Guibas. Pointnet: Deep learning on point sets for 3d classification and segmentation. In *Proceedings of the IEEE conference on computer vision and pattern recognition*, pages 652–660, 2017.
- [48] J.-W. Qian, R. Privat, J.-N. Jaubert, and P. Duchet-Suchaux. Enthalpy and heat capacity changes on mixing: fundamental aspects and prediction by means of the ppr78 cubic equation of state. *Energy & fuels*, 27(11):7150–7178, 2013.
- [49] M. Rajabi-Kochi, N. Mahboubi, A. P. S. Gill, and S. M. Moosavi. Adaptive representation of molecules and materials in bayesian optimization. *Chemical Science*, 16(13):5464–5474, 2025.
- [50] M. Ramírez-de Santiago. Viscosity of binary liquid mixtures: A comparative analysis of mixing rules. *Industrial & Engineering Chemistry Research*, 63(51):22470–22480, 2024.
- [51] S. Ravanbakhsh, J. Schneider, and B. Póczos. Deep learning with sets and point clouds. *arXiv preprint arXiv:1611.04500*, 2016.

- [52] A. Ravia, K. Snitz, D. Honigstein, M. Finkel, R. Zirler, O. Perl, L. Secundo, C. Laudamiel, D. Harel, and N. Sobel. A measure of smell enables the creation of olfactory metamers. *Nature*, 588(7836):118–123, 2020.
- [53] J. Ruza, M. Stolberg, S. Cawthorn, J. Johnson, Y. Shao-Horn, and R. Gómez-Bombarelli. Autonomous discovery of polymer electrolyte formulations with warm-start batch bayesian optimization. *arxiv*, 2025.
- [54] V. Sharma, M. Giammona, D. Zubarev, A. Tek, K. Nugyuen, L. Sundberg, D. Congiu, and Y.-H. La. Formulation graphs for mapping structure-composition of battery electrolytes to device performance. *Journal of Chemical Information and Modeling*, 63(22):6998–7010, 2023.
- [55] E. Soares, V. Sharma, E. V. Brazil, R. Cerqueira, and Y.-H. Na. Capturing formulation design of battery electrolytes with chemical large language model. In *AI for Accelerated Materials Design-NeurIPS 2023 Workshop*, 2023.
- [56] M. K. Taraday, A. David, and C. Baskin. Sequential signal mixing aggregation for message passing graph neural networks. *arXiv preprint arXiv:2409.19414*, 2024.
- [57] A. Thorat, A. K. Verma, R. Chauhan, R. Sartape, M. R. Singh, and J. K. Shah. Identifying high ionic conductivity compositions of ionic liquid electrolytes using features of the solvation environment. *Journal of Chemical Theory and Computation*, 2025.
- [58] G. Tom, C. T. Ser, E. M. Rajaonson, S. Lo, H. S. Park, B. K. Lee, and B. Sanchez-Lengeling. From molecules to mixtures: Learning representations of olfactory mixture similarity using inductive biases. *arXiv preprint arXiv:2501.16271*, 2025.
- [59] J. M. Uceda, M. Morales, M. Cartes, and A. Mejía. Experimental determination and theoretical modeling of isobaric vapor–liquid equilibria, liquid mass density, surface tension and dynamic viscosity for the methyl butyrate and tert-butanol binary mixture. *Fluid Phase Equilibria*, 587:114199, 2025.
- [60] A. Vaswani, N. Shazeer, N. Parmar, J. Uszkoreit, L. Jones, A. N. Gomez, Ł. Kaiser, and I. Polosukhin. Attention is all you need. *Advances in neural information processing systems*, 30, 2017.
- [61] R. L. Vekariya. A review of ionic liquids: Applications towards catalytic organic transformations. *Journal of Molecular Liquids*, 227:44–60, 2017.
- [62] P. V. Verdes, J. Vijande, M. M. Mato, J. L. Legido, and M. P. Andrade. Measurement and prediction of excess molar enthalpies of ternary mixtures involving ether with 1-alkanol and n-alkane. *Journal of Molecular Liquids*, 408:125323, 2024.
- [63] O. Vinyals, S. Bengio, and M. Kudlur. Order matters: Sequence to sequence for sets. *arXiv preprint arXiv:1511.06391*, 2015.
- [64] E. Wagstaff, F. Fuchs, M. Engelcke, I. Posner, and M. A. Osborne. On the limitations of representing functions on sets. In *International Conference on Machine Learning*, pages 6487–6494. PMLR, 2019.
- [65] J. Wei, D.-H. Lu, Y.-Y. Ma, A.-L. Yi, H.-X. Dong, and D.-W. Fang. Effect of temperature on the minimum excess molar volume and the molar surface gibbs energy of the binary of the ether-functionalized ionic liquids [c22o1im][scn] with monohydric alcohols at t=(288.15–318.15) k. *Journal of Molecular Liquids*, 307:112856, 2020.
- [66] T. Weiss, K. Snitz, A. Yablonka, R. M. Khan, D. Gafsou, E. Schneidman, and N. Sobel. Perceptual convergence of multi-component mixtures in olfaction implies an olfactory white. *Proceedings of the National Academy of Sciences*, 109(49):19959–19964, 2012.
- [67] U. Westhaus, T. Dröge, and R. Sass. Detherm®—a thermophysical property database. *Fluid phase equilibria*, 158:429–435, 1999.
- [68] Z. Wu, B. Ramsundar, E. N. Feinberg, J. Gomes, C. Geniesse, A. S. Pappu, K. Leswing, and V. Pande. Moleculenet: a benchmark for molecular machine learning. *Chemical science*, 9(2):513–530, 2018.

- [69] J. Xie and G. Tong. Advances in set function learning: A survey of techniques and applications. *ACM Computing Surveys*, 2025.
- [70] C. Yang, P. Ma, F. Jing, and D. Tang. Excess molar volumes, viscosities, and heat capacities for the mixtures of ethylene glycol+ water from 273.15 k to 353.15 k. *Journal of Chemical & Engineering Data*, 48(4):836–840, 2003.
- [71] Z. Yu, H. Wang, X. Kong, W. Huang, Y. Tsao, D. G. Mackanic, K. Wang, X. Wang, W. Huang, S. Choudhury, et al. Molecular design for electrolyte solvents enabling energy-dense and long-cycling lithium metal batteries. *Nature Energy*, 5(7):526–533, 2020.
- [72] M. Zaheer, S. Kottur, S. Ravanbakhsh, B. Póczos, R. R. Salakhutdinov, and A. J. Smola. Deep sets. *Advances in neural information processing systems*, 30, 2017.
- [73] J. Zang, W. Zhai, Y. Wang, B. Zhang, X. Ma, K. Ma, and J. Zhang. Excess properties, intermolecular interaction, and co₂ capture performance of diethylene glycol monomethyl ether+ ethylenediamine binary mixed solutions. *Journal of Molecular Liquids*, 417:126561, 2025.
- [74] J. Zaslavsky and C. Allen. A dataset of formulation compositions for self-emulsifying drug delivery systems. *Scientific Data*, 10(1):914, 2023.
- [75] H. Zhang, T. Lai, J. Chen, A. Manthiram, J. M. Rondinelli, and W. Chen. Learning molecular mixture property using chemistry-aware graph neural network. *PRX Energy*, 3(2):023006, 2024.
- [76] R. Zhang, J. Chen, and J. Mi. Excess molar enthalpies for binary mixtures of different amines with water. *The Journal of Chemical Thermodynamics*, 89:16–21, 2015.
- [77] W. Zhang, X. Chen, Y. Wang, L. Wu, and Y. Hu. Experimental and modeling of conductivity for electrolyte solution systems. *ACS omega*, 5(35):22465–22474, 2020.
- [78] Y. Zhang, J. Hare, and A. Prügel-Bennett. Fspool: Learning set representations with featurewise sort pooling. *arXiv preprint arXiv:1906.02795*, 2019.
- [79] Y. Zhou and J. Qu. Ionic liquids as lubricant additives: a review. *ACS applied materials & interfaces*, 9(4):3209–3222, 2017.
- [80] S. Zhu, B. Ramsundar, E. Annevelink, H. Lin, A. Dave, P.-W. Guan, K. Gering, and V. Viswanathan. Differentiable modeling and optimization of non-aqueous li-based battery electrolyte solutions using geometric deep learning. *Nature Communications*, 15(1):8649, 2024.
- [81] M. Zohair, V. Sharma, E. A. Soares, K. Nguyen, M. Giammona, L. Sundberg, A. Tek, E. A. Vital, and Y.-H. La. Chemical foundation model guided design of high ionic conductivity electrolyte formulations. *arXiv preprint arXiv:2503.14878*, 2025.
- [82] A. Zweig and J. Bruna. Exponential separations in symmetric neural networks. *Advances in Neural Information Processing Systems*, 35:33134–33145, 2022.

A Appendix

A.1 Dataset licenses

We list the different licenses of the dataset curated in CHEMIXHUB below:

- Miscible Solvent: CC BY-NC 4.0
- IIThermo: CC BY 4.0
- NIST TRC SOURCE Zenodo archive: CC BY 4.0
- Drug solubility: CC BY 4.0
- Solid polymer electrolyte: MIT
- Motor Octane Number: CC BY 4.0
- Olfactory Similarity: CC BY 4.0

A.2 Details of molecular graph representation

The GNN takes in molecular graphs derived from the SMILES representations of molecules. Each graph, written as $G = (U, V, E)$, consists of a special global vertex U connected to all other vertices V , and a set of edges E . The global vertex U encodes overall properties of the molecule and is initialized with 200 normalized RDKit descriptors obtained from DESCRIPTASTORUS [29]. The atoms of the molecules are the vertices (nodes), with node vectors $V = \{v_i\}_{i=1}^{N_v}$ for a molecule with N_v atoms, where v_i are feature vectors encoding atomic properties. Covalent bonds between atoms are represented as edges $E = \{(e_k, r_k, s_k)\}_{k=1}^{N_e}$ for a molecule with N_e bonds, where e_k are feature vectors of edge properties, and $r_k, s_k \in [1, \dots, N_v]$ are indices of the two atoms that the bond joins together. Note $r_k \neq s_k$, since bonds must be between two different atoms

The node features used in the molecular graph representation as input to the GNN are 85-dimensional one-hot encoding vectors, encoding categorical information about the atoms. The edge features encode the categorical information about the bonds as 14-dimensional one-hot encoding vectors. The molecular information for the features are shown in Table 4.

Table 4: Features for node and edge features of molecular graphs

All categories are one-hot encoded and stacked to give a singular bit vector. UNK stands for "unknown", and is a catch-all category.

Node features	Categories
Atomic number	1 (hydrogen) to 54 (iodine), UNK
Atom degree	0, 1, 2, 3, 4, 5, UNK
Formal charge	-2, -1, 0, 1, 2, UNK
Chirality	unspecified, CW, CCW, other, UNK
Number of hydrogens	0, 1, 2, 3, 4, 5, 6, 7, 8, UNK
Hybridization	sp, sp2, sp3, sp3d, sp3d2, UNK
Aromatic	True/False
Edge features	Categories
Bond type	single, double, triple, aromatic, UNK
Is conjugated	True/False
In ring	True/False
Stereo-configuration	none, Z, E, cis, trans, any, UNK

As mentioned in Section 3.3, polymers and salts are present in the dataset and this probes important modeling considerations when employing GNNs. For polymers, we decided to restrict our modeling consideration to passing their monomeric units to the GNN. For salts, we conducted a chemical analysis to determine the impact of modeling the cation and anion as one disconnected graph. The details of it can be found in Section A.10.

A.3 Compute resources details

All model training/validation was conducted on a single A100 40GB NVIDIA GPU.

A.4 Training details

Each run was performed for 500 epochs using the Adam optimizer [30], with a batch size set to 1024. Early stopping was implemented with patience set to 100. Two different learning rates were used to train the models end-to-end, one for the molecular-level model and one for the rest of the model. The splits used are specified in Section 3.4, further details on hyperparameter tuning can be found in Section A.5.

A.5 Hyperparameter search

For each task, the search was performed using Weights & Biases [5] with the BOHB algorithm [20] and a budget of 160 runs. 80 runs were allocated to the GNN-based molecular representations and 80 to CLMs and descriptors runs. Each run was performed for 500 epochs with early stopping patience set to 100. The search was conducted using the first split of the 5-fold random CV splits (70/10/20 training/validation/test split). The search space is defined as follows

- Molecular featurization: ["custom molecular graphs", "molt5 embeddings", "rdkit2d normalized features"]
- General hyper-parameters:
 - Loss type: ["mae", "mse"]
 - Dropout rate: [0, 0.05, 0.1, 0.15, 0.2, 0.25, 0.3, 0.35, 0.4, 0.45, 0.5]
 - Learning rate (molecular level): [8e-5, 5e-5, 1e-4, 5e-4, 8e-4, 1e-3, 5e-3, 1e-2]
 - Learning rate (mixture level and head): [8e-5, 5e-5, 1e-4, 5e-4, 8e-4, 1e-3, 5e-3, 1e-2]
- Molecular-level hyper-parameters:
 - Molecular context aggregation type: ["concatenate", "multiply", "film"]
 - FiLM layer activation function: ["sigmoid", "relu"]
- Mixture-level hyper-parameters:
 - Mixture interaction module: ["self attention", "deepset"]
 - MLP head in self-attention: ["True", "False"]
 - Embedding dimension: [32, 64, 96, 128]
 - Number of layers: [0, 1, 2, 3]
 - Aggregation type: ["mean", "max", "pna", "scaled pna", "attention", "set2set"]
 - Number of attention heads: [1, 4, 8, 16]
 - Output dimension: [96, 128, 256]
 - Mixture context aggregation type: ["concatenate", "film"]
 - FiLM layer activation function (mixture context): ["sigmoid", "relu"]
- Predictive head hyper-parameters:
 - Embedding dimension: [64, 128, 192, 256, 320]
 - Number of layers: [1, 2, 3]

For runs where the molecular featurization used GNNs, the following additional parameters were added to the search space:

- GNN hyper-parameters:
 - Embedding dimension: [64, 128, 192, 256, 320]
 - Number of layers: [2, 3, 4]

A.6 XGBOOST modeling

The XGBOOST model was given a maximum of 1,000 estimators and tree depth of 1,000 except for the full NIST task, where a maximum of 250 estimators and a tree depth of 250 was used. To ensure the model does not overfit, we use the validation set for early stopping, with a patience of 25 epochs. The model is trained with mean squared error, with a learning rate of 0.01.

A.7 IIThermo Dataset curation details

We use the IIThermo package to retrieve IIThermo entries, selecting entries that are either binary or ternary mixtures and corresponding to our property of choice (for the scope of this paper, we limit ourselves to viscosity and ionic conductivity properties) [26]. We remove mixture that exhibits multiple phases behavior and are not liquid at the indicated temperature. We apply a natural logarithm transformation to the viscosity and ionic conductivity values present in IIThermo to make the range of values easier to learn. We also constrain the pressure range to be near the standard value of 1 atm or 101.325 kPa by applying a ± 2 kPa threshold on pressure values.

We then standardize the mixture composition metric to mole fraction by converting as many entries as possible into that format. Data points which have the mixture composition expressed using molarity are discarded, as the conversion would require making assumption about the component densities.

Assuming a binary mixture of component A and B with a given mole ratio $r_{A:B} = \frac{n_A}{n_B}$ where n_A and n_B are the number of moles of A and B , respectively, the mole fractions χ_A and χ_B can be calculated using:

$$\chi_A = \frac{n_A}{n_A + n_B} = \frac{r_{A:B}}{r_{A:B} + 1} \quad (2)$$

$$\chi_B = 1 - \chi_A \quad (3)$$

Similarly, assuming a ternary mixture of component A , B and C with given mole ratios $r_{A:B} = \frac{n_A}{n_B}$ and $r_{A:C} = \frac{n_A}{n_C}$, the mole fractions χ_A , χ_B and χ_C can be retrieved using:

$$\chi_A = \frac{n_A}{n_A + n_B + n_C} = \frac{r_{A:B}}{r_{A:B} + \frac{r_{A:B}}{r_{A:C}} + 1} \quad (4)$$

$$\chi_B = \frac{n_B}{n_A + n_B + n_C} = \frac{\frac{1}{r_{A:B}}}{\frac{1}{r_{A:B}} + \frac{1}{r_{A:C}} + 1} \quad (5)$$

$$\chi_C = \frac{\frac{1}{r_{A:C}}}{\frac{1}{r_{A:B}} + \frac{1}{r_{A:C}} + 1} \quad (6)$$

Assuming a binary mixture of component A and B , and given the mass ratio $r_{A:B} = \frac{m_A}{m_B}$ where m_A and m_B are the mass of A and B in g, respectively and the molecular weights MW_A and MW_B , to retrieve the mole fractions χ_A and χ_B , we first calculate mass fractions γ_A and γ_B using:

$$\gamma_A = \frac{m_a}{m_a + m_b} = \frac{r_{A:B}}{r_{A:B} + 1} \quad (7)$$

$$\gamma_B = 1 - \gamma_A \quad (8)$$

then assuming $m_{tot} = m_A + m_B = 1$ g, we use $m_A = \gamma_A m_{tot}$ and $m_B = \gamma_B m_{tot}$ to obtain

$$n_A = \frac{m_A}{MW_A} \quad (9)$$

$$n_B = \frac{m_B}{MW_B} \quad (10)$$

$$n_{tot} = n_A + n_B \quad (11)$$

$$\chi_A = \frac{n_A}{n_{tot}} \quad (12)$$

$$\chi_B = 1 - \chi_A \quad (13)$$

The same process is naturally extended for ternary mixtures, assuming $r_{C:B} = \frac{m_C}{m_B}$ and MW_C are given.

Assuming a binary mixture of component A and B , and given the molarity $M_A = \frac{n_A}{m_B}$ where m_B is the mass of B in kg and n_A the number of moles of A and the molecular weights M_A and M_B , to retrieve the mole fractions χ_A and χ_B , we assume $m_B = 1$ kg so $M_A = n_A$ and use $n_B = \frac{m_B}{MW_B}$ to obtain:

$$\chi_A = \frac{n_A}{n_A + n_B} = \frac{M_A}{M_A + \frac{1000}{MW_B}} \quad (14)$$

$$\chi_B = 1 - \chi_A \quad (15)$$

where a factor of 1000 is introduced since M_A and M_B are expressed in g/mol. The same process is naturally extended for ternary mixtures, assuming $M_C = \frac{n_C}{m_B}$ and MW_C are given.

Assuming a binary mixture of component A and B , and given the weight fraction γ_A and the molecular weights M_A and M_B , to retrieve the mole fractions χ_A and χ_B , we assume $m_{tot} = m_A + m_B = 1\text{g}$ and use $m_A = \gamma_A m_{tot}$ and $m_B = \gamma_B m_{tot}$ to obtain:

$$n_A = \frac{m_A}{MW_A} = \frac{\gamma_A}{MW_A} \quad (16)$$

$$n_B = \frac{m_B}{MW_B} = \frac{\gamma_B}{MW_B} = \frac{1 - \gamma_A}{MW_B} \quad (17)$$

$$\chi_A = \frac{n_A}{n_A + n_B} \quad (18)$$

$$\chi_B = 1 - \chi_A \quad (19)$$

The same process is naturally extended for ternary mixtures, assuming γ_C and MW_C are given.

A.8 Additional metrics for performances across tasks

In addition to the MAE results reported in Section 4.2, we report the results compiled from the CV splits for all models evaluated in terms of Pearson correlation coefficient ρ and Kendall ranking coefficient τ in Table 5 and 6, respectively.

Table 5: **Model performances across CHEMIXHUB tasks** Reported Pearson correlation coefficient ρ (\uparrow) on 5-fold random CV splits. The mean and standard deviation are reported.

Molecular rep.	Mixture rep.	Miscible Solvents			Drug Solubility	SPE	NIST-full
		ρ	ΔH_{mix}	ΔH_{vap}	$\ln(S)$	$\ln(\kappa)$	$\ln(\eta)$
GNN	Attention	0.948 ± 0.076	0.974 ± 0.003	0.998 ± 0.000	0.993 ± 0.001	0.970 ± 0.004	0.980 ± 0.002
	Deepsets	0.999 ± 0.000	<u>0.974 ± 0.004</u>	0.851 ± 0.296	0.996 ± 0.001	0.969 ± 0.010	0.981 ± 0.002
MolT5	XGB	0.992 ± 0.001	0.924 ± 0.005	0.987 ± 0.001	0.999 ± 0.000	<u>0.976 ± 0.001</u>	0.989 ± 0.001
	Attention	0.998 ± 0.001	0.976 ± 0.003	0.997 ± 0.004	0.992 ± 0.005	0.973 ± 0.001	0.975 ± 0.038
	Deepsets	0.997 ± 0.001	0.976 ± 0.003	0.999 ± 0.000	0.983 ± 0.003	0.967 ± 0.002	0.977 ± 0.002
RDKit	XGB	0.992 ± 0.000	0.945 ± 0.007	0.986 ± 0.001	0.999 ± 0.000	0.977 ± 0.001	0.992 ± 0.000
	Attention	0.997 ± 0.001	0.972 ± 0.003	0.991 ± 0.003	0.996 ± 0.001	0.947 ± 0.008	0.995 ± 0.000
	Deepsets	0.996 ± 0.001	0.954 ± 0.005	0.999 ± 0.000	0.973 ± 0.004	0.963 ± 0.003	0.970 ± 0.002
Molecular rep.	Mixture rep.	IIThermo		MON	NIST	Olfaction	
		$\ln(\kappa)$	$\ln(\eta)$	MON	$\ln(\eta)$	Mixture similarity	
GNN	Attention	0.986 ± 0.008	0.975 ± 0.012	0.360 ± 0.300	<u>0.990 ± 0.002</u>	0.447 ± 0.120	
	Deepsets	0.989 ± 0.002	0.939 ± 0.060	0.820 ± 0.087	<u>0.990 ± 0.002</u>	0.132 ± 0.103	
MolT5	XGB	0.997 ± 0.000	0.995 ± 0.001	0.860 ± 0.032	0.950 ± 0.003	0.432 ± 0.047	
	Attention	0.988 ± 0.001	0.993 ± 0.003	0.893 ± 0.028	0.991 ± 0.001	0.559 ± 0.040	
	Deepsets	0.993 ± 0.002	0.986 ± 0.002	0.880 ± 0.036	0.981 ± 0.001	0.548 ± 0.025	
RDKit	XGB	0.997 ± 0.001	0.995 ± 0.001	0.913 ± 0.019	0.957 ± 0.003	0.476 ± 0.062	
	Attention	0.987 ± 0.003	0.981 ± 0.003	0.197 ± 0.351	0.977 ± 0.024	0.056 ± 0.130	
	Deepsets	0.991 ± 0.002	0.992 ± 0.001	0.752 ± 0.155	0.980 ± 0.002	-0.091 ± 0.050	

A.9 Additional benchmark

DiffMix (3 tasks) Battery electrolytes—mixtures of salts and solvents—have been optimized to facilitate ion transport, prevent electron transfer, and stabilize electrode-electrolyte interfaces to produce energy-dense and durable battery systems [71, 21]. The DiffMix dataset is a collection of three tasks centered around thermodynamic and transport properties predictions of electrolytes originally gathered by Zhu et al. [80]. This data is under the CC BY-NC-ND 4.0 license, and we therefore cannot include it as part of our dataset.

Table 6: **Model performances across CHEMIXHUB tasks** Reported Kendall ranking coefficient τ (\uparrow) on 5-fold random CV splits. The mean and standard deviation are reported.

Molecular rep.	Mixture rep.	Miscible Solvents			Drug Solubility $\ln(S)$	SPE $\ln(\kappa)$	NIST-full $\ln(\eta)$
		ρ	ΔH_{mix}	ΔH_{vap}			
GNN	Attention	0.910 ± 0.091	0.835 ± 0.004	0.969 ± 0.002	0.932 ± 0.003	0.868 ± 0.016	0.904 ± 0.007
	Deepsets	0.973 ± 0.000	0.833 ± 0.003	0.816 ± 0.318	0.949 ± 0.004	0.869 ± 0.023	0.905 ± 0.002
MolT5	XGB	0.924 ± 0.00	0.730 ± 0.008	0.897 ± 0.003	0.978 ± 0.001	0.899 ± 0.003	0.950 ± 0.000
	Attention	0.963 ± 0.006	0.835 ± 0.002	0.955 ± 0.034	0.935 ± 0.022	0.881 ± 0.003	0.956 ± 0.003
RDKit	Deepsets	0.966 ± 0.002	0.835 ± 0.002	0.976 ± 0.001	0.893 ± 0.010	0.861 ± 0.004	0.910 ± 0.004
	XGB	0.929 ± 0.002	0.773 ± 0.005	0.898 ± 0.003	0.978 ± 0.001	0.899 ± 0.004	0.966 ± 0.000
RDKit	Attention	0.961 ± 0.003	0.829 ± 0.003	0.944 ± 0.012	0.948 ± 0.006	0.840 ± 0.014	0.957 ± 0.003
	Deepsets	0.956 ± 0.001	0.788 ± 0.008	0.973 ± 0.002	0.856 ± 0.009	0.855 ± 0.007	0.921 ± 0.002
Molecular rep.	Mixture rep.	IIThermo		MON MON	NIST $\ln(\eta)$	Olfaction	
		$\ln(\kappa)$	$\ln(\eta)$			Mixture similarity	
GNN	Attention	0.923 ± 0.021	0.941 ± 0.029	0.348 ± 0.203	0.940 ± 0.007	0.312 ± 0.073	
	Deepsets	0.930 ± 0.006	0.863 ± 0.103	0.687 ± 0.093	0.942 ± 0.009	0.166 ± 0.067	
MolT5	XGB	0.974 ± 0.000	<u>0.967 ± 0.001</u>	0.756 ± 0.038	0.863 ± 0.002	0.319 ± 0.047	
	Attention	0.930 ± 0.004	<u>0.967 ± 0.010</u>	0.768 ± 0.033	0.939 ± 0.001	0.377 ± 0.042	
RDKit	Deepsets	0.942 ± 0.004	0.945 ± 0.002	0.714 ± 0.012	0.896 ± 0.001	0.390 ± 0.011	
	XGB	0.973 ± 0.001	0.968 ± 0.001	0.781 ± 0.029	0.883 ± 0.003	0.342 ± 0.040	
RDKit	Attention	0.924 ± 0.015	0.957 ± 0.000	0.164 ± 0.266	0.916 ± 0.029	0.036 ± 0.065	
	Deepsets	0.928 ± 0.005	0.956 ± 0.002	0.583 ± 0.121	0.897 ± 0.005	-0.048 ± 0.035	

Table 7: DiffMix tasks summary. *T* indicates Temperature dependency. *Mole Fractions* indicates if mole fractions of the mixture components are available. *Arrhenius relationship* indicates if the task can be modeled using the Arrhenius equation. *Exp.* indicates if the data was obtained from wet-lab experiments or simulations.

Tasks	Units	Datapoints	Max # Components	# Unique Mixtures	# Unique Molecules	Mixture Context	Mole Fractions	Arrhenius Relationship	Exp.
DiffMix	κ	mS/cm	24,822	4	82	8	T	✓	✗
	ΔV	cm ³ /mol	1069	2	28	25	T	✓	✓
	H_m^E	kJ/mol	631	2	34	35	T	✓	✓

- **Excess molar enthalpy H_m^E :** The excess molar enthalpy reflects changes in intermolecular interactions that occur during the mixing of different components [76]. It shows the non-ideality of the final solution and gives an explanation about enthalpic effects [48]. In particular, differences in molecular shape, size, and interaction types between components—along with variations in temperature and pressure—can lead to either an increase or a decrease in excess molar enthalpy [35, 62]. DiffMix dataset includes 631 H_m^E data points curated from literature, covering 34 unique mixtures composed of 35 organic compounds across varying compositions. We rescaled the original range of the DiffMix excess molar enthalpy task from J/mol to kJ/mol to avoid passing big values to the neural networks.
- **Excess molar volume V_m^E :** The excess molar volume represents the deviation from ideal mixing volume. It exhibits a non-linear dependence on mole fraction [10] and temperature [65]—often showing a U-shaped trend with concentration and a decrease in absolute values as temperature increases. At higher temperatures, the dependence may shift to an S-shaped profile, making accurate prediction particularly challenging [70]. DiffMix dataset includes 1069 V_m^E data points curated from literature, covering 28 unique mixtures composed of 25 organic compounds.
- **Ionic conductivity κ :** The ionic conductivity of the electrolyte is known as a key parameter to evaluate the performance of the solution in practical engineering applications. In the context of batteries, κ changes considerably with the change of the electrolyte concentration [77]. DiffMix dataset includes 24,822 mixtures of single-salt-ternary-solvent electrolyte solutions generated using Advanced Electrolyte Model [22], and covering arbitrary combinations of two unique salts and six organic carbonate solvents at different concentration.

Table 8: **Model performances across CHEMIXHUB tasks** on 5-fold random CV splits. The mean and standard deviation are reported.

(a) MAE (\downarrow)				
Molecular rep.	Mixture rep.	DiffMix		
		κ	V_m^E	H_m^E
GNN	Attention	0.205 ± 0.061	0.060 ± 0.004	0.029 ± 0.006
	Deepsets	0.306 ± 0.054	0.072 ± 0.004	0.062 ± 0.014
MolT5	XGB	0.059 ± 0.002	0.042 ± 0.007	0.042 ± 0.004
	Attention	0.167 ± 0.164	0.056 ± 0.005	<u>0.023 ± 0.003</u>
	Deepsets	0.046 ± 0.006	0.062 ± 0.005	0.021 ± 0.002
RDKit	XGB	0.050 ± 0.001	0.045 ± 0.00	0.045 ± 0.006
	Attention	0.168 ± 0.064	0.079 ± 0.008	0.251 ± 0.123
	Deepsets	0.110 ± 0.011	0.074 ± 0.005	0.090 ± 0.065
(b) Pearson ρ (\uparrow)				
Molecular rep.	Mixture rep.	DiffMix		
		κ	V_m^E	H_m^E
GNN	Attention	0.993 ± 0.004	0.950 ± 0.005	0.996 ± 0.004
	Deepsets	0.984 ± 0.007	0.946 ± 0.007	0.982 ± 0.006
MolT5	XGB	0.998 ± 0.000	0.933 ± 0.023	0.989 ± 0.003
	Attention	0.994 ± 0.010	0.950 ± 0.008	<u>0.998 ± 0.001</u>
	Deepsets	1.000 ± 0.000	0.949 ± 0.009	0.998 ± 0.000
RDKit	XGB	0.999 ± 0.000	0.932 ± 0.026	0.983 ± 0.010
	Attention	0.995 ± 0.003	0.944 ± 0.005	0.422 ± 0.378
	Deepsets	0.998 ± 0.000	0.945 ± 0.006	0.964 ± 0.052
(c) Kendall τ (\uparrow)				
Molecular rep.	Mixture rep.	DiffMix		
		κ	V_m^E	H_m^E
GNN	Attention	0.929 ± 0.019	0.873 ± 0.023	0.928 ± 0.028
	Deepsets	0.887 ± 0.013	0.863 ± 0.026	0.852 ± 0.031
MolT5	XGB	0.973 ± 0.002	0.901 ± 0.025	0.909 ± 0.026
	Attention	0.948 ± 0.039	0.890 ± 0.022	<u>0.957 ± 0.005</u>
	Deepsets	0.983 ± 0.002	0.881 ± 0.023	0.957 ± 0.002
RDKit	XGB	0.980 ± 0.001	0.900 ± 0.025	0.903 ± 0.012
	Attention	0.945 ± 0.015	0.838 ± 0.045	0.472 ± 0.257
	Deepsets	0.954 ± 0.006	0.850 ± 0.027	0.828 ± 0.098

A.10 Modeling salts

Salts are often present in mixtures, these are non-bonded small molecules that are found in the same environment as the molecule. To explore how to properly model salts we first look at if they contribute meaningfully to basic featurizations.

We constructed a 200-dimensional molecular embedding space using RDKit 2D descriptors obtained from DESCRIPTASORUS [29], incorporating both salts and fragments for all the tasks in CHEMIXHUB. The number of unique salts is 824, and the number of fragments is 476. This space was projected into two dimensions using UMAP to visualize structural relationships, Figure 5. As shown in the UMAP plot, The resulting plot shows that salts (blue triangles) and fragments (orange circles) broadly co-localize, with many salts embedded near fragment clusters.

To quantify these observations, we computed cosine distances between each salt and the fragment-only descriptor space. The resulting distribution confirms that the vast majority of salts lie within a narrow cosine distance range centered around 0.04–0.05, with very few exceeding 0.1, Figure 6. In RDKit descriptor space, such low distances imply near-identity in structural features.

From these, we can observe that most salts appear to retain descriptor-level similarity to their constituent fragments. However, there is a subset which introduces structural changes significant enough to shift them away from the fragment space.

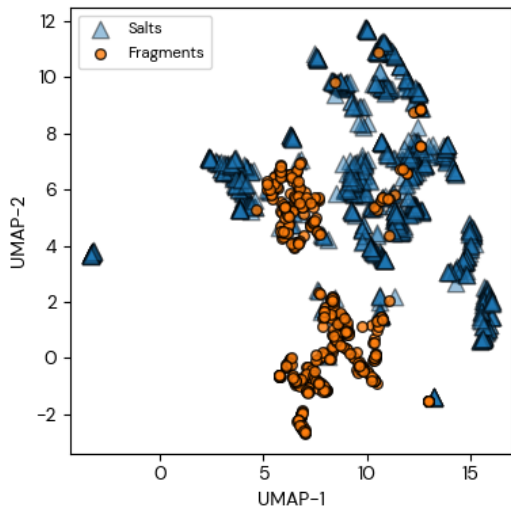


Figure 5: **The embedding space of salts and fragments in CHEMIXHUB.** UMAP projection of the combined RDKit 2D descriptor space (200 dimensions) for salts and fragments. The embedding reveals well-defined structural clusters with apparent separation between salts and fragments, rather than overlap. Most salts appear in peripheral regions relative to the fragment clusters, suggesting distinct structural patterns at the descriptor level.

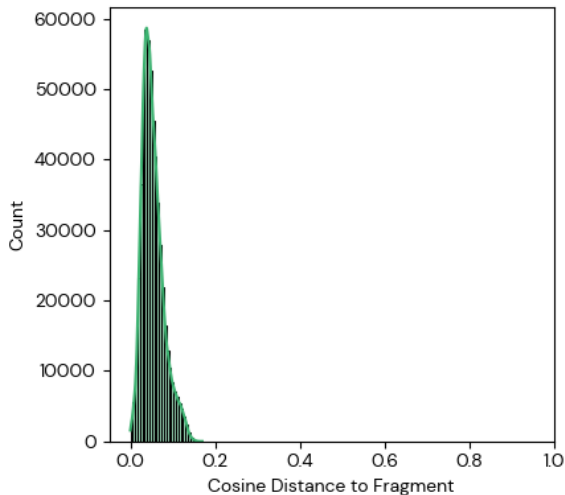


Figure 6: **Distribution of cosine distances.** The majority of salts fall within a tight cosine distance range (centered around 0.04–0.05), indicating strong structural similarity at the descriptor level. A smaller subset of salts shows higher distances, suggesting meaningful deviations from fragment-like chemistry.

Based on this analysis we conclude that most basic featurizations do not properly model salts. We think the best way to currently model salts is either as disconnected nodes in a graph. When using a

GRAPHNETS architecture, these disconnected nodes get routed to the globals, so they are roughly equivalent to learnable salt-specific embeddings at the globals level of the graph.